IEEE Access
Multidisciplinary | Rapid Review | Open Access Journal

Received January 16, 2020, accepted February 5, 2020, date of publication February 12, 2020, date of current version February 26, 2020.

Digital Object Identifier 10.1109/ACCESS.2020.2973458

Topology-Preserving and Geometric Feature-Correction Watermarking of Vector Maps

XU XI[1], XINCHANG ZHANG[2], YING SUN[1], XIN JIANG[1], AND QINCHUAN XIN[1]

[1]School of Geography and Planning, Sun Yat-sen University, Guangzhou 510275, China
[2]School of Geographical Sciences, Guangzhou University, Guangzhou 510006, China

Corresponding author: Ying Sun (sunying23@mail.sysu.edu.cn)

This work was supported in part by the National Key Research and Development Program of China under Grant 2018YFB2100702, in part by the National Natural Science Foundation of China under Grant 41671453 and Grant 41431178, in part by the Natural Science Foundation of Guangdong Province, China, under Grant 2016A030311016, in part by the National Administration of Surveying, Mapping and Geoinformation of China, under Grant GZIT2016-A5-147, in part by the Research Institute of Henan Spatio-Temporal Big Data Industrial Technology under Grant 2017DJA001, and in part by the Fundamental Research Funds for the Central Universities under Grant 19lgpy44.

ABSTRACT Digital watermarking is an effective method of vector map copyright protection. However, the topology and geometric features are potentially influenced by the disturbances of vertices caused by watermark embedding, thus reducing the availability of watermarked vector maps. In this research, we propose a post-correction method for two-dimensional vector map watermarking, by which the topology and geometric features of the input data can be preserved, while using only conventional watermarking techniques. In the proposed method, the Maximum Perturbation Regions (MPR) of vertices and direction angle constraints methods of adjacent lines are adopted to undergo multi-azimuth checks of watermarked vertices, which may cause changes of the geometric features and topology. After that, the coordinate adjustment method which is based on the homonymous vertices topology association and the MPR are combined for topology and geometric feature correction. For watermark embedding, two classic frequency domain watermarking techniques, Discrete Fourier Transformation (DFT) and Discrete Wavelet Transformation (DWT), phase based and low-frequency coefficient based respectively, are also adopted. The scheme was conducted on a building vector map and a road vector map. The experimental results show that the proposed method can ensure the topology consistency and geometric feature similarity of vector maps before and after embedding watermarks. Moreover, this method has little interference with the maps, which improves the usability of the watermarked vector map.

INDEX TERMS Watermark, vector map, maximum perturbation region (MPR), topology-preserving, geometric feature-correction.

I. INTRODUCTION

As an important strategic resource for the national economy, national defense construction, and social development, vector maps may feature accurate and detailed geographical coordinates, expensive production costs, prominent economic or military interests, etc., [1]–[3]. However, vector maps are easily copied, tampered with, or illegally spread, and this can seriously damage the legitimate rights and interests of data owners. In recent years, digital watermark technology has become an effective method of vector map copyright protection [4].

Vector map watermarking algorithms usually include three steps: watermark generation, watermark embedding, and watermark detection [5], [6], and they come in two flavors, according to the embedding location of the watermark: (1) coordinate domain watermarking algorithms; and (2) frequency domain watermarking algorithms. Cox and Jager [7] first proposed the coordinate domain watermarking algorithm for vector maps, which advocates directly encoding watermark information on each vertex coordinate. The bits of the embedded watermark information are uncorrelated, and they

The associate editor coordinating the review of this manuscript and approving it for publication was Wu-Shiung Feng.

are not robust against various simple attacks [8]. The LSB (Least Significant Bit) based method is a very classic idea in coordinate domain watermarking [9]–[11], which embeds the watermark information in the coordinate precision bit. The method is of high computational efficiency; however, it is vulnerable to precision bit erasure. Studies researches of coordinate domain watermarking usually embedded watermarks by controlling the tolerances, position, and precision of the elements in the vector map [12]–[16]. These methods have a good performance for maintaining accuracy; however, the robustness against geometric attacks is one-sided. Recently, coordinate domain watermarking for vector data has begun to focus on the geographical features, geometric shapes, topological relations, and layer structures of elements. Shao *et al.* [17] embedded watermark information in the distance sequence of feature points. This method can maintain the shape of the elements in the vector map to a certain extent; however, it is not resistant to noise superposition. The vector map watermarking algorithm proposed by Wang *et al.* [18], based on polygon topological relation, is robust against rotation, scaling and translation transformation (RST), simplification, and noise superposition. Nevertheless, it is weak to resist data cropping and is difficult apply to vector maps with more polylines than polygons (such as contour maps and road maps). Yang [19] proposed a watermark embedding strategy that took into account spatial constraints. However, the scheme cannot guarantee the usability of vector map after watermark embedding, and it is necessary to add the corresponding spatial constraints into the embedding process. Tong *et al.* [20] embedded watermark information in the angle value constituted by adjacent vertices in the vector map, which improved the watermark capacity and reduced the interference to the data by compression and reconstruction of watermark information. However, this method has a poor ability in compression resistance and point deletion. Wang *et al.* [21] mapped the vertices to the logic domain and divided the logic domain into blocks according to the number of watermarks, and embedded watermarks in each block, in order to realize multiple watermark embedding. The method has strong robustness against clipping attacks, but poor ability against rotation, scaling, translation. Overall, coordinate domain watermarking for vector map embedding watermark are under the control of accuracy tolerance. However, they are often of less robustness as the watermark information can be easily eliminated by targeted attacks.

Different from the coordinate domain watermarking, frequency domain watermarking embeds a watermark by modifying the transform coefficients rather than the coordinate values of the vertices. Typical frequency domain algorithms include the discrete Fourier transform (DFT), the discrete wavelet transform (DWT), and the discrete cosine transform (DCT) [22]. Wang *et al.* [23] embedded the watermark on the DFT phase. In their research, the robustness of watermarking was improved by using the phases' strong resistance to point deletion, format conversion and RST attacks. Xu *et al.* [24] improved the watermarking's ability to resist geometric attacks, by combining the invariance of amplitude and phase of DFT and embedded watermarks in the amplitude and phase, at the same time. Yang and Zhu [25] and Sangita and Parvatham [26] considered the insensitivity of low wavelet coefficients to data changes, and adopted similar strategies to embed watermark in the low-frequency coefficients of DWT. Voigt *et al.* [27] proposed a reversible watermarking algorithm for 2D vector data based on DCT. The algorithm made use of the high correlation between the vertices of the same polygon. The watermark information was embedded on the cosine transform coefficient of each data block composed of every eight vertices. Although this algorithm is reversible, it may easily to cause geometric deformation of the vector graphics. Overall, frequency domain watermarking is more widely used than coordinate domain watermarking, yet unescapable defects remain: The embedding positions in the vertices have great randomness, and the embedding strength is uncontrollable [3], [28]. Moreover, most of the frequency domain watermarking studies have focused on the method effectiveness and confidentiality, ignoring the availability of the watermarked vector map. On the whole, the vector map watermarking scheme should not only have the basic features of a general digital watermarking algorithm, but also meet the higher requirements of data accuracy, topological structure, geometric features, and other spatial features.

In view of this, the detection and correction of topology change and geometric feature loss caused by coordinate perturbation are the key elements in the frequency domain watermarking. Abubahia and Cocea [29] proposed a metric for measuring the topological quality of watermarked vector maps, but lack of consideration about topology correction. Huber *et al.* [30] detected and corrected the vertices where topological errors occurred after watermark embedding. They calculated the maximum perturbation region (MPR) of each vertex by the Voronoi diagram and constrained triangulations. After embedding the watermark, the vertices beyond the MPRs would be forcibly moved to the edge of the MPRs to maintain the topology of the vector map. However, the method only focused on maintaining topology, ignoring the loss of geometric features. In this study, we propose a post-correction method for two-dimensional vector map watermarking that can maintain both the consistency of topology and the similarity of geometric features. The objectives of this study are to: (1) detect the topology errors and geometric feature changes of watermarked vector map by MPR and direction constraint; (2) modify the vertices where topology and geometric feature changes occurred, using the coordinate adjustment method based on the homonymous vertices topology association. The watermarks are embedded into the vector map by DFT-based and DWT-based watermarking schemes.

II. METHODOLOGY

The method proposed for the better maintenance of both topology and geometric features in vector map watermarking,

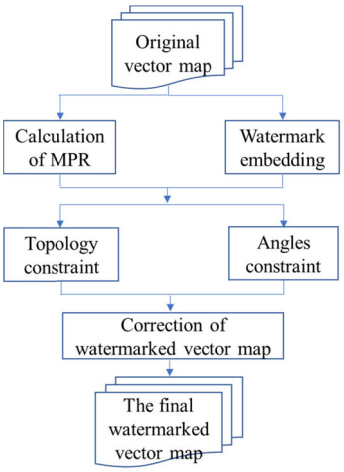

FIGURE 1. The vector map watermarking framework.

as shown in Figure 1, mainly consists of three parts. First, the MPR is used for topology constraints to detect and eliminate the topology errors, such as edge crossing. Secondly, the direction constraint of the adjacent polyline of the same vertex is considered to detect and keep the geometric features of map elements. Finally, a coordinate adjustment method based on the homonymous vertices topology association is employed for error vertex correction (hereafter referred to as a dirty vertex).

Before embedding the watermark, the MPR of each vertex in the vector map is calculated, and then two typical watermarking algorithms, named DFT based watermarking and DWT based watermarking are used to embed watermarks in the vector map to obtain the watermarked vector map. In view of the topology errors or geometric feature loss that occurred in the process of watermark embedding, the MPR is used to detect possible dirty vertices. Then, the direction constraint and topology constraint are used to check the dirty vertices to obtain the set of vertices with topology errors or excessive angle changes. Finally, the coordinate adjustment method based on topology association of the same vertex is adopted to adjust the dirty vertices into the MPRs or at the position that meets constraint conditions, so as to eliminate topology errors or geometric feature loss caused by watermark embedding on the vector map. After the correction, the final watermarked vector map is obtained.

A. CALCULATION OF THE MPR

The original vector map can be donated as $G = (V, E)$ with a vertex set $V = \{v_1, v_2, \ldots, v_n\}$, where $v_i \in \mathbb{R}^2$, and an edge set E. The process of watermark embedding can be expressed as a mapping $\varphi : V \to \mathbb{R}^2$ that perturbs each vertex of G. The watermarked vector map can be denoted as $G' = (V', E)$ with the watermarked vertex set $V' = \{\varphi(v_i) : v_i \in V\}$. The process of finding the maximum perturbation regions (MPRs) $R_1, R_2, \ldots, R_n$, with $v_i \in R_i \subset \mathbb{R}^2$, is to hold the following property: If $\varphi(v_i) \in R_i$ for all $1 \le i \le n$ then containment relations and all incidence orders hold for G'. In other words,

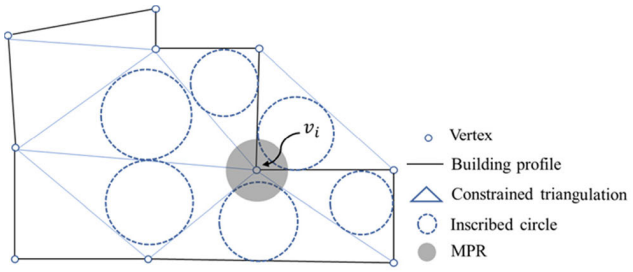

FIGURE 2. The triangulation-based approach: R_I is equal to the minimum radius of its triangle, incident to v_i.

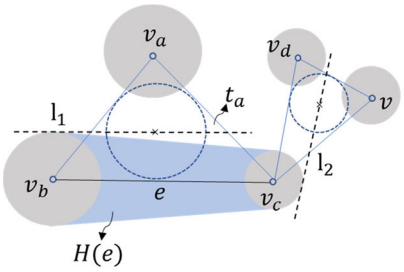

FIGURE 3. Case of the proof of Theorem 1: The MPR of v_a cannot intersect $H(e)$, as a separating line exists.

$R_1, R_2, \ldots, R_n$ are safe regions for the corresponding vertices without changes in the input topology after the perturbation from embedding watermarks. More terminologies and notations used, but not clearly explained in this work can referred to in [31]–[35].

The constrained Delaunay triangulation network is adopted to calculate MPRs: $R_i (i = 1, 2, \ldots, n)$ (FIGURE 2). First, the constraint Delaunay triangulation network T of vector map G is constructed, t_i represents a triangle in T, and $I(t_i)$ is the radius of the inscribed circle corresponding to the triangle. Then, we calculate the smallest radius of the inscribed circle in all adjacent triangles of vertex v_i, and take it as the radius length of R_i, so that the MPR (geometric circle with the center of v_i) of a vertex can be obtained. Hence, R_i of v_i can be obtained as:

$$R_i = Circle_{v_i}(r_i) \tag{1}$$

where, $r_i = \min_{1 \le j \le d_i} I(t_i^j)$, with t_i^j denoting all triangles incident to v_i, and d_i is the number of adjacent triangles.

Theorem 1: If the perturbation v_i' of the vertex $v_i \in V$ is constrained to R_i, as defined in (1) *, for $1 \le i \le n$, then the topology is guaranteed for G'.*

Proof of Theorem 1: We let v_a be a vertex such that (v_a, v_b, v_c) forms a triangle, t_a of T, and define a hose, $H(e)$, for a circular arc, e, with endpoints v_b and v_c, see Figure 3. In fact, $H(e)$ represents the valid area in which the perturbed edge $v_b'v_c'$ may lie. As can be seen from Figure 2, T is a triangulation of the vertices of G, such that each edge of G is also an edge of T. To establish Theorem 1, we must prove that no MPR at a node v intersects a hose $H(e)$. By construction, the radii of the MPRs at v_a, v_b, and v_c are less than or, at most, equal to the radius of $I(t_a)$. Now consider a line, l_1, through

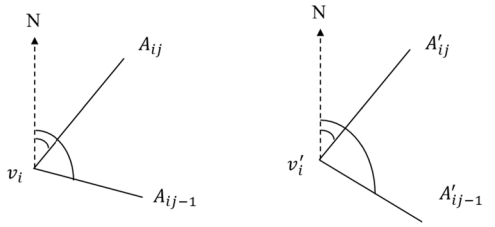

FIGURE 4. The direction constraints diagram.

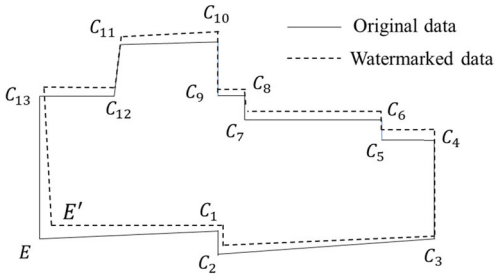

FIGURE 5. The polygon before and after watermark embedding.

the center of the incircle of t_a that is parallel to e. We see that $H(e)$ lies completely within one closed half-plane induced by l_1, while the MPR around v_a lies completely within the other open half-plane. We concluded that the MPR around v_a and the hose $H(e)$ do not overlap or touch if the vertices of e and v_a form a triangle of T. In particular, the orientation of (v'_a, v'_b, v'_c) is the same as the orientation of (v_a, v_b, v_c). By applying this argument repeatedly to all triangles we learn that there is no non-trivial intersection between an MPR and a hose. In summary, the topology can be guaranteed.

B. DIRECTION CONSTRAINTS FOR THE ADJACENT LINES

In order to guarantee that the geometric shapes of a vector map are similar after embedding a watermark, we adopt the direction constraint method [36], to constrain the angle deviation degree of adjacent lines. In this article, we specified the due north direction of 0°, increasing clockwise, and the direction of each line should be calculated respectively to measure the angles between vertex joint lines, the range of line direction angle is [0°–360°].

FIGURE 4 shows the homonymous vertices v_i and v'_i, in which v_i is the vertex of the vector map and v'_i is the same vertex after watermark embedding. Here, we employ the direction constraint method to judge whether v'_i a dirty vertex. We suppose that the v_i joint lines are $\{A_{i1}, A_{i2}, \ldots, A_{ij}\}$, and the v'_i joint lines are $\{A'_{i1}, A'_{i2}, \ldots, A'_{ij}\}$, and treat v_i and v'_i as origins (as shown in Figure 3). If the direction change degree is larger than the threshold (2), v'_i needs direction adjustment:

$$\left|dir(A_{ij} - A'_{ij})\right| \leq \theta; \quad j = 1, 2, 3, \ldots. \tag{2}$$

where dir is the calculation function for the line directions, and θ is the threshold, which determines whether the geometric feature loss occurred. During the experiment, we found that the link vertices of the line segments are all within the MPRs if the θ value is less than 3°, and the geometry is similar to the original data. However, the link vertices are not necessarily within the MPRs if the threshold value is greater than 3°, and the corresponding line segments show obvious geometric changes. Accordingly, we consider that the geometric features change when the angle change (θ) between adjacent lines is greater than 3° after watermark embedding, and that the geometrical features of ground objects have to be adjusted in this study.

C. COORDINATE ADJUSTMENT METHOD BASED ON THE HOMONYMOUS VERTICES TOPOLOGY ASSOCIATION

For the vertices that violate topology constraints (vertices that are outside of MPRs and generate errors such as boundary intersection, etc., and can be checked by common topology tools) or violate direction constraints, we adopt the coordinate adjustment method based on the homonymous vertices topology association for correction [37]. FIGURE 5 shows a polygon (solid line), which is constituted with a vertices sequence, $\{E, C_1, C_2, \ldots, C_{13}\}$, and the corresponding vertices sequence, $\{E', C'_1, C'_2, \ldots, C'_{13}\}$, after embedding the watermark (dotted line). Assuming that the vertex E' is a dirty vertex, which has a topology error or geometric distortion, while the rest are correct ones. The coordinate adjustment method based on the homonymous vertices topology association, can be employed to calculate the coordinate adjustment amount of E'.

First, we use the breadth-first search algorithm to traverse the entire vector map to determine which correct vertices are associated with the dirty vertices. Specifically, the search area can be regarded as a tree with the current node (dirty vertex) as the root node. The determination of the influence range is actually to determine a subtree with the current node as the root, and the other correct vertices are treated as leaf nodes of the subtree. Therefore, if the breadth-first search algorithm starts with the root node, the traversal is completed when all correct vertices in the subtree are added to the influence range (vertex set) of the current vertex.

As the subtree is traversed, the path from the root node to a correct vertex is recorded to determine the impact of the correct vertex on the dirty vertex. The smaller the distance between two vertices, the greater the adjustment effect on the dirty vertex. Therefore, we take the reciprocal of distance as the influence weight, that is, $W = 1/D$, where D is the Euclidean distance between the correct vertex and the 'dirty vertex'. The specific coordinate adjustment can be obtained from the following equation:

$$\begin{cases} \Delta X_E = \sum_{i=1}^{n} \Delta X_{Ci} \dfrac{w_i}{\sum_{j=1}^{n} w_j} \\ \Delta Y_E = \sum_{i=1}^{n} \Delta Y_{Ci} \dfrac{w_i}{\sum_{j=1}^{n} w_j} \end{cases} \tag{3}$$

where $(\Delta X_E, \Delta Y_E)$ is the dirty vertex coordinate adjustment amount, $C_i (i = 1, 2, \ldots, n)$ represents all correct vertices

that are associated with the dirty vertex, n is the number of the correct vertices, and the change quantity in coordinates at each of the correct vertex is $(\Delta X_{Ci}, \Delta Y_{Ci})$.

D. TWO TYPICAL FREQUENCY DOMAIN WATERMARKING ALGORITHMS FOR VECTOR MAPS

In order to verify the effectiveness of the vector map watermarking processing scheme proposed in this paper, two kinds of watermarking algorithms [23], [26] based on DFT and DWT, were used for the experiments. On this basis, the possible topology errors or geometric feature loss caused by these two watermarking algorithms are checked and corrected. The basic embedding strategies are as follows:

1) WANG'S METHOD: DFT-BASED WATERMARKING

The DFT based watermarking [23] is a commonly used scheme due to the unique advantages in resisting geometric attacks. The specific watermark embedding process is as follows: The binary watermark sequence is denoted as $W = \{w_m = 0, 1 \,|m = 0, 1, \ldots, N-1\}$, where N represents the length of the watermark sequence. For the convenience of watermark extraction, the 0 in w_m needs to be converted to -1. After the conversion, $W = \{w_m = \pm 1 \,|m = 0, 1, \ldots, N-1\}$.

We transform the original vertex sequence $\{v_k = (x_k, y_k)\}$ in the vector map to a complex sequence with the equation:

$$a_k = x_k + i * y_k \tag{4}$$

where x_k and y_k are horizontal coordinates and vertical coordinates of the k th vertex, respectively. a_k is a complex sequence. We perform a discrete Fourier transform on a_k, and the DFT coefficients can be obtained with equation (5):

$$A_l = \frac{1}{N} \sum_{k=0}^{N-1} a_k (e^{-2\pi i / N})^{kl}, \quad l \in [0, N-1] \tag{5}$$

The DFT coefficients of sequence A_l contain the amplitude $\{|A_l|\}$ and phase $\{\angle A_l\}$.Then, watermark information is added to the phase sequence according to the addition rule. The watermark embedding algorithm is described as follows:

$$\angle A'_l = A_l + \rho * w_m \tag{6}$$

where ρ is the embedding strength.

Combined with watermarked phase, $\angle A'_l$, and amplitude, $|A_l|$, to perform inverse discrete Fourier transformation (IDFT), we can get the watermarked complex sequence $a'_k = x'_k + i * y'_k$. We can obtain the watermarked vector map G' by fixing the ordinate values of the vertices according to a'_k.

The flow chart of DFT-based watermarking is shown in FIGURE 6. The watermark extraction is the inverse process of watermark embedding.

2) SANGITA'S METHOD: THE DWT-BASED WATERMARKING

In DWT-based watermarking [26], the high-frequency coefficient can be treated as noise. The high-frequency coefficient

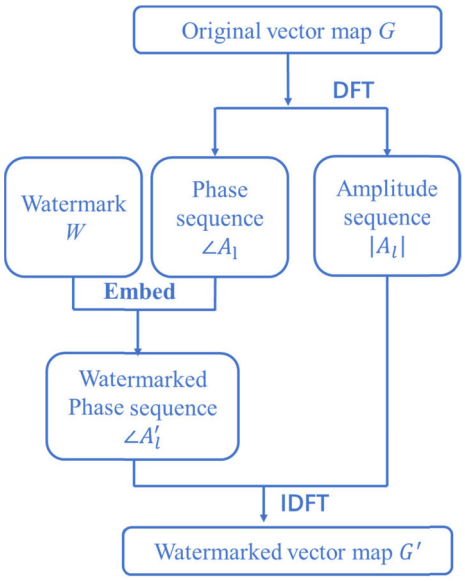

FIGURE 6. Schematic flow of watermark embedding for discrete Fourier transformation (DFT) based watermarking.

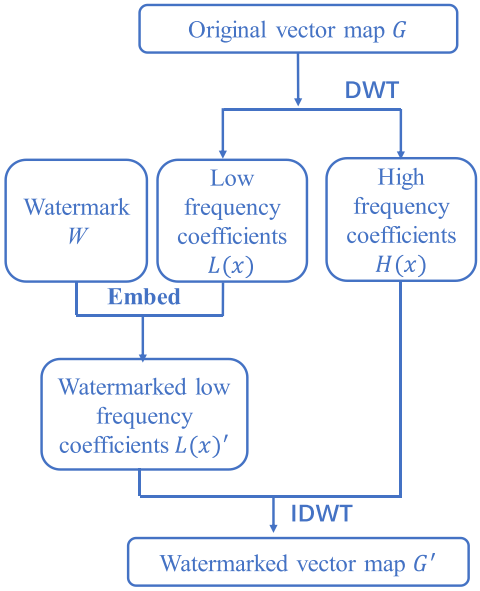

FIGURE 7. Schematic flow of watermark embedding for discrete wavelet transformation (DWT) based watermarking.

usually clearly changed with the vector map, while the low-frequency coefficient has better stability. Therefore, embedding the watermark information in a DWT low-frequency coefficient would have good resistance against noise [25].

The basic embedding strategy is shown in FIGURE 7: A two-layer discrete wavelet transform is applied on the original vertex sequence $\{v_k = (x_k, y_k)\}$. We can obtain the four coefficients HH2, LH2, HL2 and LL2. Only low-frequency coefficients (LL2) are considered for watermark embedding denoted as $L(x)$. The watermark embedding algorithm is described as follows:

$$L(x)' = L(x) + \rho * w_m \tag{7}$$

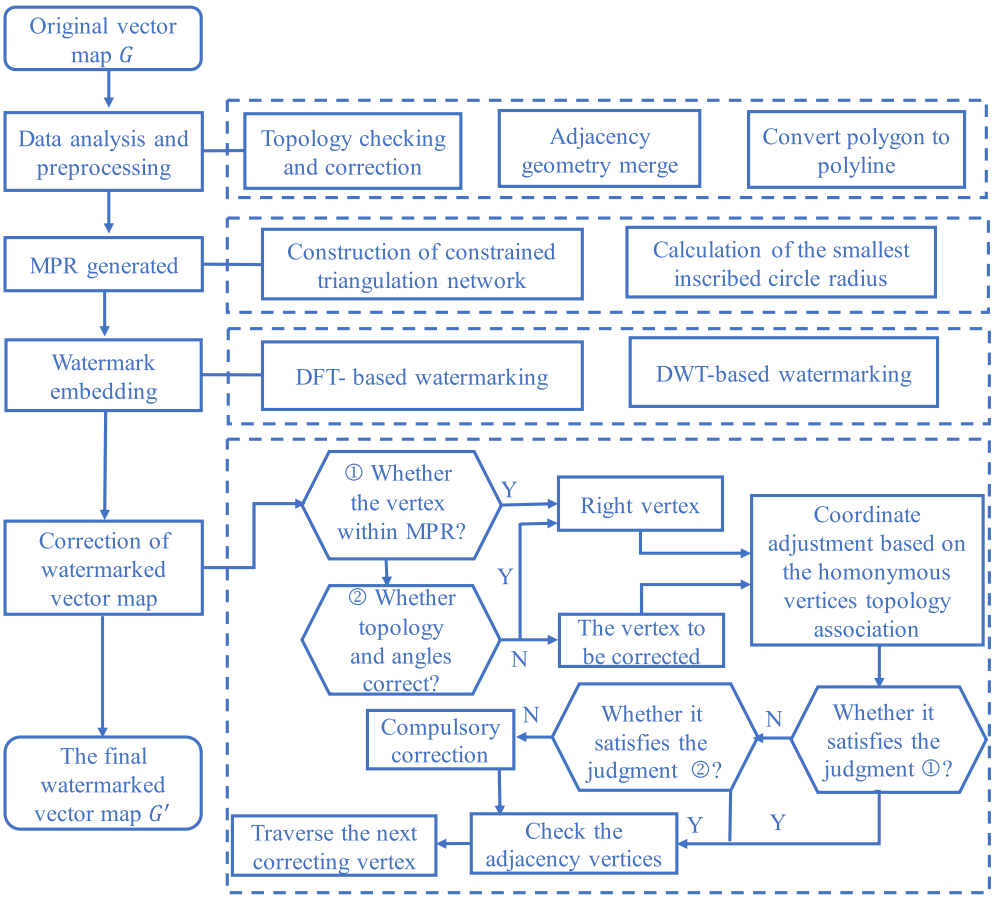

FIGURE 8. The flowcharts for our method of preserving topology and geometric features of watermarked vector maps.

Then, the watermarked low frequency coefficients, $L(x)'$, are performed inverse discrete wavelet transformation (IDWT) with other three unwatermarked coefficients, thereby obtaining a watermarked vector map. The flow chart in FIGURE 7 shows the two most important coefficients.

E. THE PROCESS OF VECTOR MAP WATERMARKING AND DATA CORRECTION

This section will elaborate on the implementation steps of the proposed method, which preserves the topology and geometric features after watermark embedding. The main process is shown in FIGURE 8:

Input: Original vector map G; watermark information w_m.

Output: Watermarked vector map G' with the same topology as, and similar geometric features to G.

Step 1: Calculating the MPR of each vertex over the original vector map G.

Step 2: Embedding the watermark information w_m into G by using the two watermarking algorithms mentioned in part D of section II to obtain the watermarked vector map G'.

Step 3. Judge the watermarked vertices as to whether they are dirty vertices. If the watermarked vertices are located in MPRs, the topology and the geometric features are well preserved. Otherwise, it is necessary to detect and correct the dirty vertices that may have topology errors or geometric feature loss. The detection for dirty vertices mainly relies on the judgement of whether the vertex violates the topology constraint or direction constraint. Among them, the topology constraint requires judgement of whether the lines intersect with other elements or itself in the process of watermark embedding, while the direction constraint requires to the judgement of whether the direction angle change of the vertex joint lines exceeds the threshold.

Step 4. Adjustment of dirty vertices. For the dirty vertex E', the coordinate adjustment method based on the same vertex topology association would be adopted to correct it. After correction, if E' is within the MPR, the topology and geometric shape of the vertex are well preserved. However, if it is still outside the MPR, the vertex would be forcibly shifted into MPR to satisfy topology and direction constraints.

Step 5. Repeat Step 3, detecting the adjacent vertices of the corrected vertex. If there are still dirty vertices, we can correct them by using Step 4. Repeat the above steps until all vertices satisfy topology and direction constraints.

Step 6. The watermarked vector map G' is finally output.

In the proposed watermarking framework, the vector maps before and after embedding watermarks will keep the topology and maintain the similarity of geometric features. For more terminologies and notations used, but not clearly explained in this work, the reader can refer to [38]–[46].

F. ASSESSMENT

The experimental results are assessed from two aspects. First, we detect the watermark information of the watermarked vector map before and after correction (we verify the influence of the correction scheme proposed in this paper on the watermark information embedded in the vector map). Secondly, we evaluate the quality of the watermarked vector map before and after correction, including topological relationship correctness, geometric similarity and data accuracy of the corrected watermarked vector map.

1) WATERMARK SIMILARITY TEST

Watermark inspection needs to make comparisons between the extracted and original watermarks. The normalized correlation (*NC*) coefficients are used to assess the similarity between watermark images as follows [47]:

$$NC = \frac{\sum_{ij} W_{ij} * W'_{ij}}{\sqrt{\sum_{ij} W_{ij}^2}\sqrt{\sum_{ij} W_{ij}'^2}} \tag{8}$$

where W_{ij} and W'_{ij} are original and extracted watermarks at the coordinates of (i, j), respectively.

2) THE CHANGE RATE ASSESSMENT OF GEOMETRIC SHAPES

The attributes such as length, area and angle are important features of linear objects and polygon objects in vector maps. In order to assess the disturbance of our correction algorithm to the watermarked vector map, we calculate the maximum change rate of the polygon angle, the change rate of the polygon perimeter and the change rate of the polygon area by comparing the uncorrected watermarked data and the corrected watermarked data with the original vector data [48].

Supposing a polygon has m edges, and the vertices coordinates set is $p_k = (x_k, y_k)$, where $k = 1, 2, \ldots, m, m+1$, $p_{m+1} = p_m$. The angle between the line segment, p_1p_2, and the line segment p_2p_3 is calculated as follows:

$$\alpha_i = arctan\left|\frac{k_i - k_{i+1}}{1 + k_i k_{i+1}}\right| \tag{9}$$

where $k_i = \frac{y_{i+1}-y_i}{x_{i+1}-x_i}$, $i = 1, 2, \cdots, m$. Based on this, the maximum change rate of this polygon angle can be obtained by the equation:

$$\alpha_{max} = \max\left(\left|\frac{\alpha'_i - \alpha_i}{\alpha_i}\right|\right) \tag{10}$$

where α'_i is the angle of the watermarked polygon. The equations for calculating the perimeter and change rate of the polygon perimeter are as follows:

$$C = \sum_{i=1}^{k}\sqrt{(x_{k+1} - x_k)^2 + (y_{k+1} - y_k)} \tag{11}$$

$$\nabla_C = \left|\frac{C' - C}{C}\right| \tag{12}$$

where S and S' are areas of the original polygon and the watermarked polygon, respectively. ∇_S is the change rate of the polygon area.

3) THE EVALUATION METHOD OF DATA ACCURACY

The watermark embedding caused a certain coordinate error between the watermarked data and the original data (13). To verify the error of the watermarked data and the effect of the proposed correction method, the mean error (*MNE*), maximum error (*ME*), mean square error (*MSE*) and signal-to-noise ratio (*SNR*) are calculated for all the vertices to evaluate the change of coordinate error before and after embedding the watermark [48].

$$e_i = \sqrt{(x_i - x'_i)^2 + (y_i - y'_i)^2} \tag{13}$$

where e_i is the coordinate error of the i-th vertex after watermark embedding. Based on e_i, the *MNE* and *ME* can be expressed as:

$$MNE = \frac{\sum_{i=1}^{n} e_i}{n} \tag{14}$$

$$ME = \max(e_i), \quad (i = 1, 2, \ldots, n) \tag{15}$$

The *MSE* and *SNR* are calculated as follows:

$$MSE = \frac{\sum_{i=1}^{n}\left[\left(x_i - x_i^{'}\right)^2 + \left(y_i - y_i^{'}\right)^2\right]}{n} \tag{16}$$

$$SNR = 10ln\frac{\sigma}{\sqrt{MSE}} \tag{17}$$

where $\sigma = \sqrt{\frac{\sum_{i=1}^{n}[(x_i - \bar{x'_i}) + (y_i - \bar{y'_i})]}{n}}$, and $\bar{x'_i} = \frac{\sum_{i=1}^{n} x_i^{'}}{n}$, $\bar{y'_i} = \frac{\sum_{i=1}^{n} y_i^{'}}{n}$.

III. STUDY MATERIALS AND DATA PREPROCESSING

The experimental data used in this paper are a building vector map of ShenZhen, Guangdong province, China and a road vector map of GuangZhou, Guangdong province, China (FIGURE 9(a, b)), which consist of polygon data and polyline data, respectively. We use SZ and GZ to represent these two data sets. The number of polygons in SZ is 1145 and the number of polylines in GZ is 3636. For SZ, embedding a watermark would change the coordinates and cause deviation of the elements in the vector map, and thus lead to the overlapping or void of the adjacent buildings. To avoid this, it is necessary to fuse all adjacent building polygons so that the common lines are eliminated, and then extract the vertices of the fused polygons, common edges and polygonal boundary lines. Meanwhile, the fused building data should be converted into line data in order to calculate the MPR region of each vertex effectively, using the constrained Delaunay

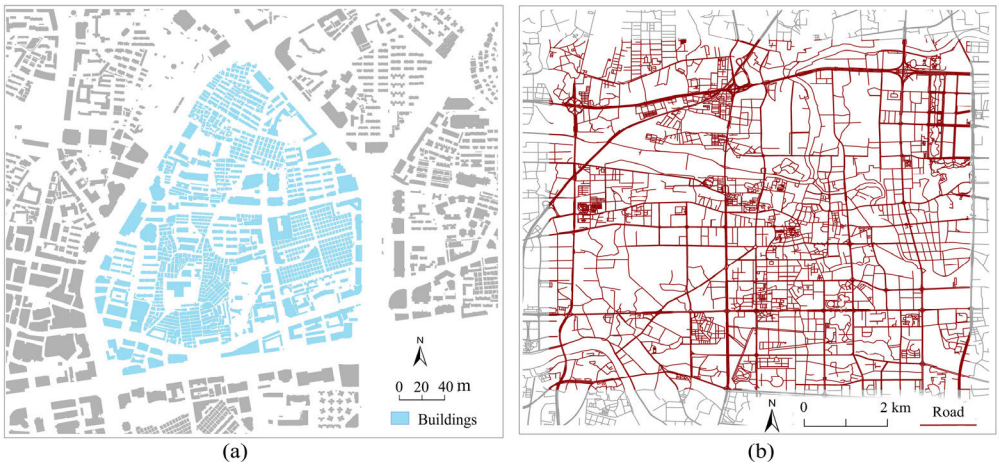

FIGURE 9. Experimental data. (a) Building vector map of ShenZhen (SZ); (b) Road vector map of GuangZhou (GZ).

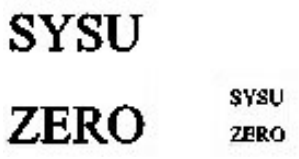

FIGURE 10. Watermark images.

triangulation method. After fusion and transformation, there are 16,247 vertices in SZ and 15,164 vertices in GZ.

The watermarks used in the experiment are shown in FIGURE. 10. They are binary images with the size of 80×80 and 32×32 containing the copyright information of 'SYSU ZERO'. To ensure the versatility of different watermarking scheme on the same data source, we implement different watermark embedding methods in the same vector map. Different watermarking schemes vary greatly in capacity, and they embed watermarks with different lengths. In the DFT-based watermarking scheme, each vertex can embed one bit of watermark information, whereas it is only 1/16 bit/vertex in a two-layer decomposition of the DWT-based watermarking scheme. Given the selected vector map, DWT-based watermarking cannot embed a complete watermark with a bit length of 6400 (80×80), while DFT-based watermarking can embed two integral 6400-length watermarks. Considering the computational efficiency and similar integral watermarks embedded for different watermarking schemes, we use the DFT-based watermarking scheme to embed 6400-length watermark, and the DWT-based watermarking scheme to embed 1024-length watermark.

IV. RESULTS AND DISCUSSION

A. GENERATION OF MPR

As is shown in FIGURE 11, we constructed a constrained Delaunay triangulation based on all vertices and calculated the inscribed circles as well as their radius in all triangles. The radius of the smallest inscribed circle connected to the vertex

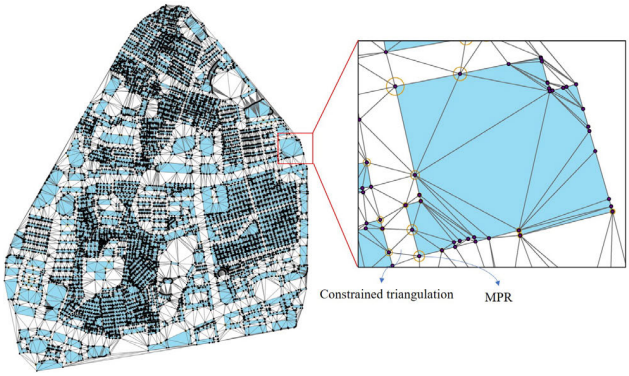

FIGURE 11. The maximum perturbation regions (MPRs) of vertices. We show SZ as the example.

is the MPR of this vertex. It can be seen from the figure that dense vertices generate small MPRs, which influences the operability of the watermark embedding. This study employs as many vertices as possible for watermark embedding, so as to investigate how the watermarking scheme influences the vertices and explore the versatility of the proposed correction scheme.

B. WATERMARK EMBEDDING AND DATA CORRECTION

The watermark information is embedded in the pre-processed building vector data using the typical vector map frequency domain watermarking algorithm based on DFT and DWT, as introduced in Section 2.4. The results are shown in FIGURE 12, FIGURE 13 and FIGURE 14. Table 1 shows the amount of watermark embedding vertex in the two watermarking algorithms, the number of vertices outside the MPRs, and the number of vertices to be corrected.

1) DFT-BASED VECTOR MAP WATERMARKING

The number of vertices in the vector maps used in this experiment are about 2.5 times the length of the watermark information. Therefore, multiple watermark

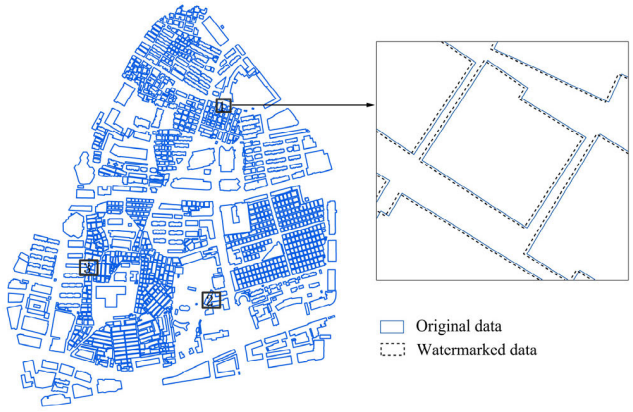

FIGURE 12. Overlay vector maps of the original data and the watermarked data. We show SZ as the example.

TABLE 1. The comparison of determining the dirty vertices.

Watermarking	Data set	Watermarked vertices	Dirty Vertices determined by [30]	Dirty Vertices determined by our method
DFT-based watermarking	SZ	16247	1067	35
	GZ	15164	1350	12
DWT-based watermarking	SZ	16247	2957	550
	GZ	15164	168	6

Note: the dirty vertices determined by reference [30] represents all the vertices outside MPRs, while we did constrain check and only vertices violating constrains were identified as dirty vertices.

information is repeatedly embedded in the DFT-based watermarking scheme, and the watermark embedding strength is 0.00005 in SZ and 0.0003 in GZ. FIGURE 12 shows the superposition of the original map and the watermarked vector map. Point displacement occurred in the watermarked vector map. During the experiment, there were 1067 vertices outside the MPRs in SZ and 1350 vertices outside the MPRs in GZ. These vertices are further checked by the topological constraints and direction constraints. In SZ, 35 vertices and in SZ,12 vertices in GZ failed to meet the constraints. These dirty vertices are corrected by the coordinate adjustment method based on the homonymous vertices topology association proposed in this paper.

FIGURE 13a and FIGURE 13b show a case of line crossing caused by watermarking in SZ. It is corrected effectively by our proposed correction method (FIGURE 13c), and the modified dirty vertices can well satisfy the topology constraint. Angle deformation (FIGURE 13d) is another outcome of watermarking, which caused geometric feature loss of the building. FIGURE 13e shows the results corrected by our method, and the geometric features are automatically recovered.

2) DWT-BASED VECTOR MAP WATERMARKING

We performed a two-layer wavelet transform and embedded watermark information in the low-frequency coefficients (LL2) with an embedded strength of 0.5 in both SZ and GZ. We can see from FIGURE 14 that there is an obvious geometric loss in SZ after the watermark embedding. As is shown in TABLE 1, the DWT-based watermarking scheme caused 2957 vertices outside the MPRs in SZ, and 168 vertices outside the MPRs in GZ. Among these, 550 vertices in SZ and six vertices in GZ did not satisfy the topological constraints and angle constraints. FIGURE 14b and FIGURE 14c show a case of angle deformation and the modified watermarked

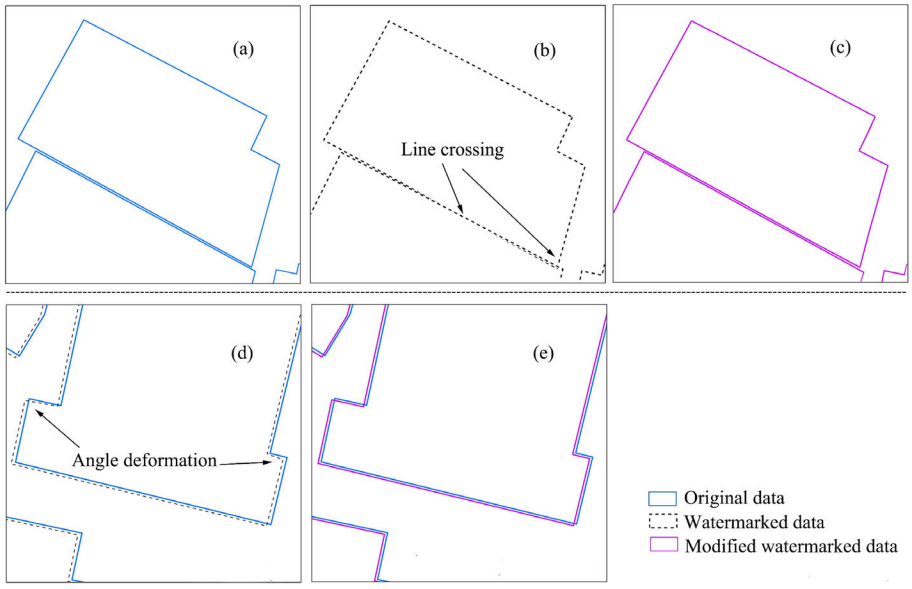

FIGURE 13. The watermarking embedding and corrected results of DWT-based watermarking. (a), (b), (c) occurred in the place marked 3 in FIGURE 12; and (d), (e) occurred in the place marked 2 in FIGURE 12.

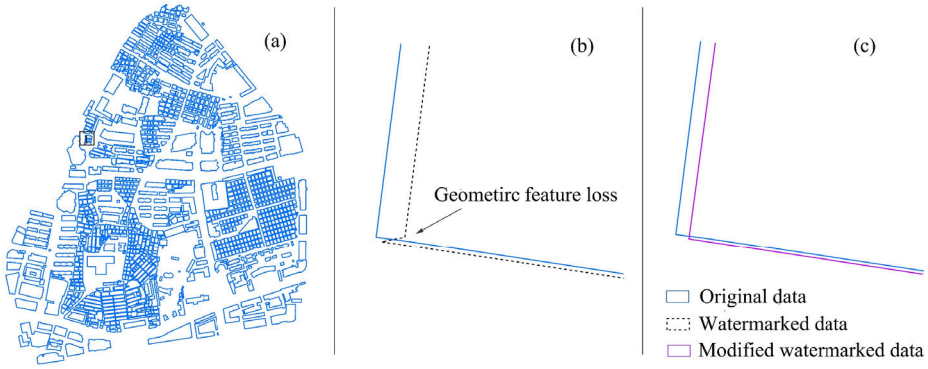

FIGURE 14. The watermarking embedding and corrected results of DWT-based watermarking in SZ. (b), (c) occurred in the place marked 1 in (a).

TABLE 2. Watermark extraction results.

Watermarking	Data set	The extracted watermark before correction	The extracted watermark after correction
DFT-based watermarking	SZ	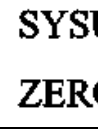	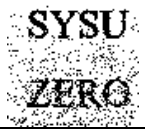
		NC=1	*NC*=0.9476
	GZ	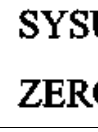	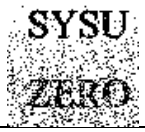
		NC=1	*NC*=0.9251
DWT-based watermarking	SZ	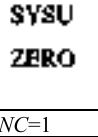	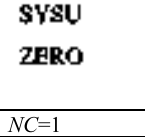
		NC=1	*NC*=1
	GZ	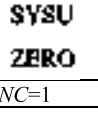	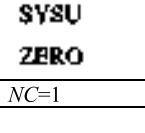
		NC=1	*NC*=1

data in SZ. The results indicate that our correction method is effective in preserving topology and geometric features after watermark embedding.

3) DETECTION OF WATERMARK INFORMATION

A criterion for testing the watermarking schemes is whether the embedded watermark information can be well detected. The normalized correlation (NC) coefficient is employed to assess the similarity between the extracted watermark image and the original watermark image. Table 2 shows the original watermark, and the extracted watermarks after the two kinds of watermarking processes on SZ and GZ, and the extracted watermarks after correction. The similarities between the original watermarks and extracted watermarks after watermarking are both 1 in the two watermarking methods before correction. After correction, the similarity reduced a little (0.9476 and 0.9251) in terms of the DFT-based watermarked maps, while it remained unchanged in the DWT-based watermarked maps.

The post-correction method is an adjustment operation after watermark embedding with certain compulsion. The robustness of the watermarking schemes have no effect on the post-correction. Contrariwise, the post-correction operation may have some impact on the watermarking scheme. The correction operation adjusts the watermarked vertices and is an attack on the watermarking. As we only adjusted a small number of vertices, and only by a small amount of magnitude, there is almost no effect on a watermarking scheme with strong robustness (the DWT-based watermarking scheme), and there may be some slight effects on a watermarking scheme with relatively weak robustness (the DFT-based watermarking scheme). The experimental results of the extracted watermark data also confirmed this view. In general, the more robust the watermarking scheme is, the impossibility that the disturbed vertices are outside the MPRs is stronger. Under such conditions, our post-correction method is more meaningful.

4) ASSESSMENT

The corrected watermarked maps are assessed from three aspects, i.e., topology checking, geometric feature assessment, and data accuracy. The topology checking of the corrected watermarked data was conducted with the topology tool in ArcMap. The results of topology checking show no topological conflict in the corrected watermarked maps, which indicates that our corrected method can well maintain the topological relationships of the vector data. FIGURE 15 shows the geometric feature assessment of SZ, and FIGURE 16 shows the geometric feature assessment of GZ. The perimeter Change rates of the two watermarked algorithms are shown in FIGURE 15a,15b and FIGURE 16a, 16b.

Taking the main change interval as a reference, the corrected perimeter change rate of SZ is slightly better than the data before the correction, while there nearly no changes for GZ. In terms of the area change rate (FIGURE 15c and 15d) and the angle change rates

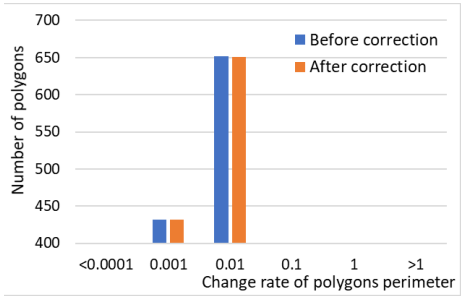

(a) Perimeter change rate in DFT-based watermarking

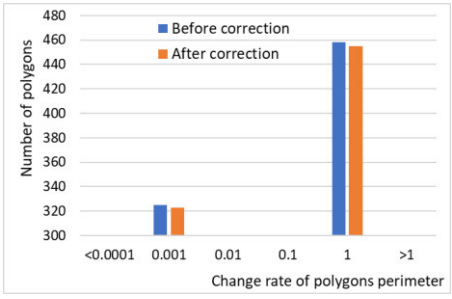

(b) Perimeter change rate of DWT-based watermarking

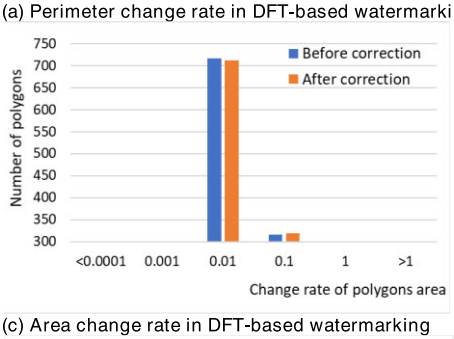

(c) Area change rate in DFT-based watermarking

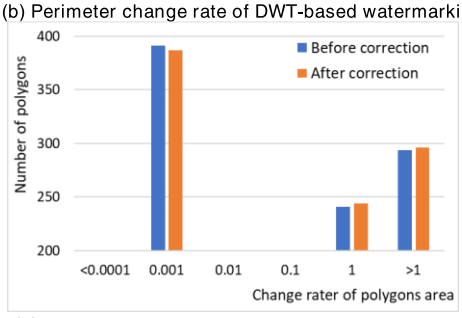

(d) Area change rate in DWT-based watermarking

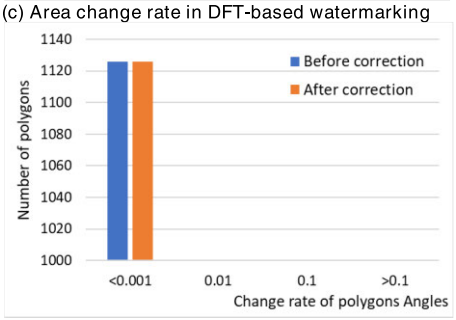

(f) Angle change rate in DFT-based watermarking

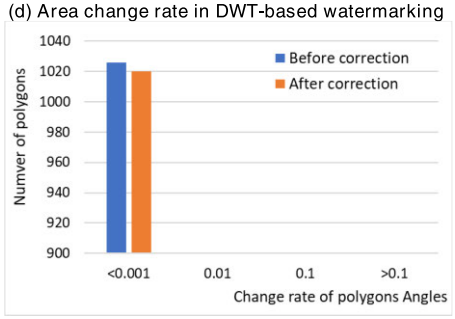

(e) Angle change rate in DWT-based watermarking

FIGURE 15. Charts of the geometry evaluation of the watermarked SZ before and after correction.

(FIGURE 15e and 15f), there are no obvious changes before and after the correction of GZ. The area change rate is not included in the evaluation of GZ, as there is no independent closed polygon in the linear data. There is a significant change in the angle change rate on DWT-based watermarking of GZ. As shown in FIGURE 16c and 16d, the polyline number in the interval 0.01–0.1 decreased after correction, while the polyline number in the interval 0.01–0.1 increased a lot. This is important evidence for our correction of geometric features. Although the change rates of the angles before and after correction in DFT- based watermarking are almost the same, our correction scheme adjusts many angles that changed greatly, to bring it closer to the original image.

Combined with the vertex perturbation results in TABLE 1 and the extracted watermark results in TABLE 2, the results satisfy the balance characteristic of the invisibility and robustness of the robust watermarking scheme. Table 3 reports the data precision of the watermarked data and corrected watermarked data. The *MNE* and *MSE* are slightly decreased in both data sets and both watermarking, while the *ME* slightly decreased in both SZ and GZ, under the DFT-based watermarking and DWT-based watermarking, which is considered as a change of the local non-feature vertices. The *SNR* is slightly improved in SZ and slightly decreased in GZ after the correction process. Overall, the correction scheme proposed in this study has very little disturbance to the vector maps,

TABLE 3. The data precision analysis of the watermarked data and the corrected data.

Watermarked data set		*MNE*	*ME*	*MSE*	*SNR*
SZ(DFT)	before correction	0.1544	0.3211	0.0271	76.0090
	after correction	0.1496	0.3211	0.0262	76.1693
SZ(DWT)	before correction	0.1250	0.1250	0.0156	78.7613
	after correction	0.1234	0.2500	0.0155	78.7860
GZ(DFT)	before correction	1.1289	2.3096	1.4954	81.1173
	after correction	1.1293	2.6095	1.4968	81.1128
GZ(DWT)	before correction	0.25	0.25	0.0625	96.9923
	after correction	0.2499	0.50	0.0625	96.9922

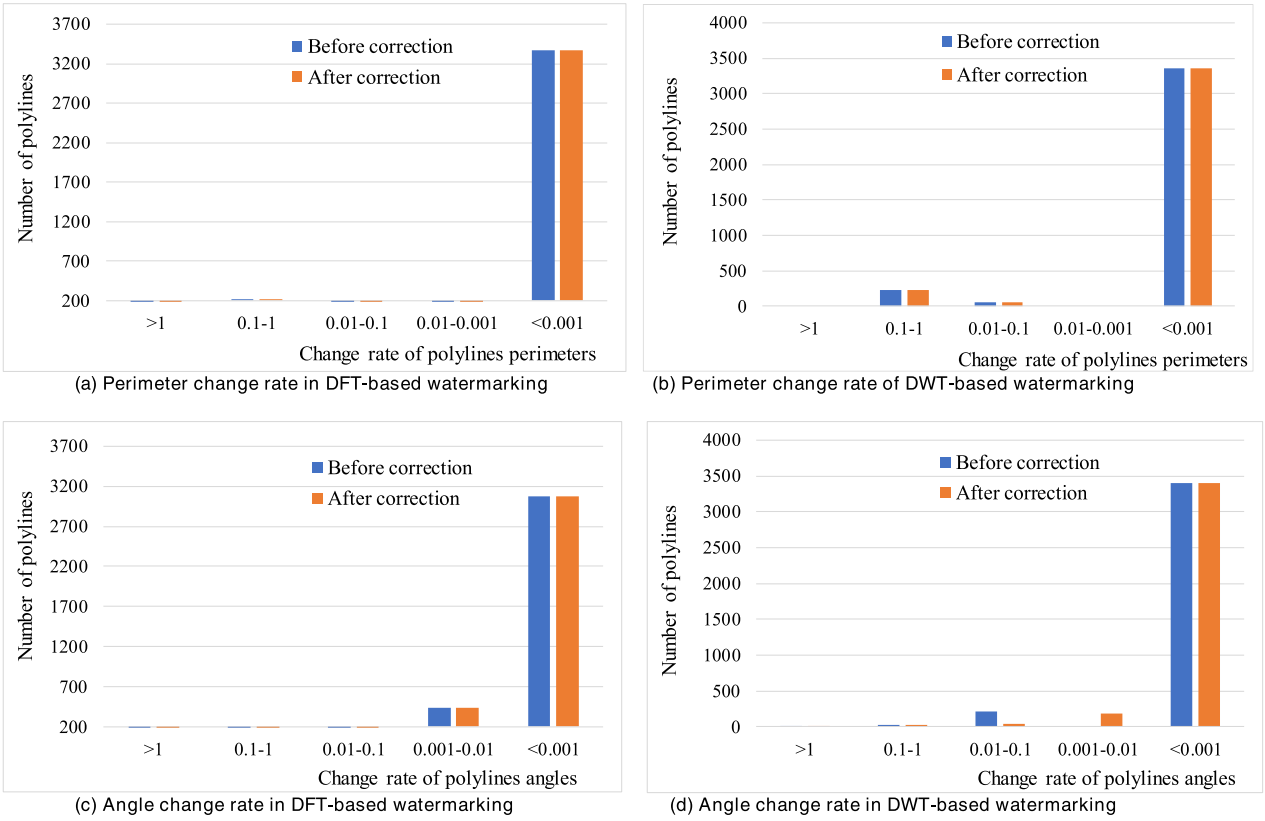

FIGURE 16. Charts of the geometry evaluation of the watermarked GZ before and after correction.

while ensuring topological consistency and geometric similarity, which ensures the fidelity and usability of the vector maps.

V. CONCLUSION

Aiming at the problem of topology change and geometric features loss after the watermark embedding in a vector map, a post-correction method has been proposed in this paper. The method adopts topology constraints and direction constrains to conduct the multi-azimuth check for the vertices which are out of the maximum perturbation regions, then MPR and a coordinate adjustment method, based on the homonymous vertices topology association, are combined to correct the dirty vertices. In this paper, the watermark embedding was carried out using the DFT and DWT-based watermarking schemes for building outline and road vector data. A building vector map of Shenzhen and a road vector map of Guangzhou were used for our method evaluation. The correction results of the watermarked data indicated that the proposed correction method can effectively maintain the topology and geometric features of the watermarked vector maps. The limitation of the proposed method is that the MPR region calculated based on the constrained Delaunay triangulation network, is relatively small, so the number of dirty vertices is much smaller than the number of vertices outside the MPRs. There are very few dirty vertices that were moved to the edge of MPRs by force, which may be over-adjusted. We will develop a more reasonable and scientific MPR calculation method in the future research.

REFERENCES

[1] C. Yang and C. Zhu, "Robust watermarking algorithm for geometrical transform for vector geo-spatial data based on invariant function," *Acta Geodaetica Cartograph. Sinica*, vol. 40, no. 2, pp. 256–261, 2011.

[2] C. Zhu, "Research progresses in digital watermarking and encryption control for geographical data," *Acta Geodaetica Cartograph. Sinica*, vol. 46, no. 10, pp. 1609–1619, 2017.

[3] A. Abubahia and M. Cocea, "Advancements in GIS map copyright protection schemes—A critical review," *Multimedia Tools Appl.*, vol. 76, no. 10, pp. 12205–12231, May 2017.

[4] R. Ohbuchi, H. Ueda, and S. Endoh, "Robust watermarking of vector digital maps," in *Proc. IEEE Int. Conf. Multimedia Expo*, Lausanne, Switzerland, Jun. 2002, pp. 577–580.

[5] N. S. Kamaruddin, A. Kamsin, L. Y. Por, and H. Rahman, "A review of text watermarking: Theory, methods, and applications," *IEEE Access*, vol. 6, pp. 8011–8028, 2018.

[6] S. Sun, Z. Lu, and X. Niu, Digital watermarking technology and Application. Beijing, China: Science Press, 2004.

[7] G. S. Cox and G. D. Jager, "A survey of point pattern matching techniques and a new approach to point pattern recognition," in *Proc. South African Symp. Commun. Signal Process.*, Cape Town, South Africa, Jan. 1992, pp. 243–248.

[8] C. Zhu, D. Xu, N. Ren, and L. Min, *Digital Watermarking Theory and Approach of Geospatial Data*. Beijing, China: Science Press, 2014.

[9] R. B. Wolfgang and E. J. Delp, "Fragile watermarking using the VW2D watermark," *Proc. SPIE*, vol. 3657, pp. 204–213, Apr. 1999.

[10] R. G. V. Schyndel, A. Z. Tirkel, and C. F. Osborne, "A digital watermark," in *Proc. IEEE Int. Conf. Image Process.*, Dec. 1994, pp. 86–90.

[11] R. K. Singh, D. K. Shaw, and M. J. Alam, "Experimental studies of LSB watermarking with different noise," *Procedia Comput. Sci.*, vol. 54, pp. 612–620, 2015.
[12] M. Sakamoto, Y. Matsuura, and Y. Takashima, "A scheme of digital watermarking for geographical map data," in *Proc. Symp. Cryptogr. Inf. Secur.*, Okinawa, Japan, 2000, pp. 26–28.
[13] G. Schulz and M. Voigt, "A high capacity watermarking system for digital maps," in *Proc. Multimedia Secur. Workshop Multimedia Secur.*, Magdeburg, Germany, 2004, pp. 180–186.
[14] S.-H. Lee and K.-R. Kwon, "Vector watermarking scheme for GIS vector map management," *Multimedia Tools Appl.*, vol. 63, no. 3, pp. 757–790, Apr. 2013.
[15] N. Wang and X. Zhao, "2D vector map data hiding with directional relations preservation between points," *AEU-Int. J. Electron. Commun.*, vol. 71, pp. 118–124, Jan. 2017.
[16] Q. Zhou, N. Ren, C. Zhu, and D. Tong, "Storage feature-based watermarking algorithm with coordinate values preservation for vector line data," *KSII Trans. Internet Inf. Syst.*, vol. 12, no. 7, pp. 3475–3496, 2018.
[17] C. Shao, H. Wang, X. Niu, and X. Wang, "Shape-preserving algorithm for watermarking 2-D vector map data," in *Proc. IEEE Multimedia Signal Process.*, Oct. 2005, pp. 1–4.
[18] C. Wang, Z. Peng, Y. Peng, L. Yu, J. Wang, and Q. Zhao, "Watermarking geographical data on spatial topological relations," *Multimedia Tools Appl.*, vol. 57, no. 1, pp. 67–89, Mar. 2012.
[19] C. Yang, "Research on the watermarking models and algorithms for vector geographic data," Ph.D. dissertation, PLA Inf. Eng. Univ., Zhengzhou, China, 2011.
[20] D. Tong, C. Zhu, and N. Ren, "Watermarking algorithm applying to small amount of vector geographical data," *Acta Geodaetica Cartograph. Sinica*, vol. 47, pp. 1518–1525, Nov. 2018.
[21] Y. Wang, C. Yang, and C. Zhu, "A multiple watermarking algorithm for vector geographic data based on coordinate mapping and domain subdivision," *Multimedia Tools Appl.*, vol. 77, no. 15, pp. 19261–19279, Aug. 2018.
[22] X. Xi, X. Zhang, W. Liang, Q. Xin, and P. Zhang, "Dual zero-watermarking scheme for two-dimensional vector map based on delaunay triangle mesh and singular value decomposition," *Appl. Sci.*, vol. 9, no. 4, p. 642, Feb. 2019.
[23] Q. Wang, C. Zhu, and D. Xu, "Watermarking algorithm for vector geospatial data based on DFT Phase," *Geomatics Inf. Sci. Wuhan Univ.*, vol. 36, no. 5, pp. 523–526, 2011.
[24] D. Xu, C. Zhu, and Q. Wang, "A construction of digital watermarking model for the vector geospatial data based on magnitude and phase of DFT," *J. Beijing Univ. Posts Telecommun.*, vol. 34, no. 5, pp. 25–28, 2011.
[25] C. Yang and C. Zhu, "Watermarking algorithm for vector geo-spatial data on wavelet transformation," *J. Zhengzhou Inst. Surveying Mapping*, vol. 24, no. 1, pp. 37–39, 2007.
[26] Z. C. Sangita and V. Parvatham, "Protecting geospatial data using digital watermarking," in *Proc. Int. Conf. Comput. Commun. Eng. (ICCCE)*, Kuala Lumpur, Malaysia, 2012, pp. 594–598.
[27] M. Voigt, B. Yang, and C. Busch, "Reversible watermarking of 2D-vector data," in *Proc. Workshop Multimedia Secur.*, Magdeburg, Germany, 2004, pp. 160–165.
[28] N. H. Barnouti, Z. S. Saabri, and K. L. Hameed, "Digital watermarking based on DWT (discrete wavelet transform) and DCT (discrete cosine transform)," *Int. J. Eng. Technol.*, vol. 7, no. 4, pp. 4825–4829, 2018.
[29] A. Abubahia and M. Cocea, "Evaluating the topological quality of watermarked vector maps," *Appl. Soft Comput.*, vol. 71, pp. 849–860, Oct. 2018.
[30] S. Huber, M. Held, P. Meerwald, and R. Kwitt, "Topology-preserving watermarking of vector graphics," *Int. J. Comput. Geometry Appl.*, vol. 24, no. 01, pp. 61–86, Mar. 2014.
[31] W. Gao, D. Dimitrov, and H. Abdo, "Tight independent set neighborhood union condition for fractional critical deleted graphs and ID deleted graphs," *Discrete Continuous Dyn. Syst.-S*, vol. 12, nos. 4–5, pp. 711–721, 2019.
[32] W. Gao, L. G. G. Juan, B. Basavanagoud, and J. Wu, "Partial multi-dividing ontology learning algorithm," *Inf. Sci.*, vol. 467, pp. 35–58, Oct. 2018.
[33] W. Gao, W. Wang, D. Dimitrov, and Y. Wang, "Nano properties analysis via fourth multiplicative ABC indicator calculating," *Arabian J. Chem.*, vol. 11, no. 6, pp. 793–801, Sep. 2018.
[34] W. Gao, H. Wu, M. K. Siddiqui, and A. Q. Baig, "Study of biological networks using graph theory," *Saudi J. Biol. Sci.*, vol. 25, no. 6, pp. 1212–1219, Sep. 2018.
[35] W. Gao, J. L. G. Guirao, M. Adbel-Aty, and W. Xi, "An independent set degree condition for fractional critical deleted graphs," *Discrete Continuous Dyn. Syst.-S*, vol. 12, nos. 4–5, pp. 877–886, 2019.
[36] M. Deng, K. Xu, B. Zhao, and R. Xu, "A hierarchical approach for nodes matching based on structural spatial relations," *Geomatics Inf. Sci. Wuhan Univ.*, vol. 35, no. 8, pp. 913–916, 2010.
[37] Q. Zhang, D. Li, and J. Gong, "The conflation of geometric data among urban geographic databases," *Bull. Surv. Mapping*, vol. 9, no. 9, pp. 27–29, 2003.
[38] W. Qiao, K. Huang, M. Azimi, and S. Han, "A novel hybrid prediction model for hourly gas consumption in supply side based on improved whale optimization algorithm and relevance vector machine," *IEEE Access*, vol. 7, pp. 88218–88230, 2019.
[39] W. Qiao, W. Tian, Y. Tian, Q. Yang, Y. Wang, and J. Zhang, "The forecasting of PM2.5 using a hybrid model based on wavelet transform and an improved deep learning algorithm," *IEEE Access*, vol. 7, pp. 142814–142825, 2019.
[40] W. Qiao and Z. Yang, "Forecast the electricity price of U.S. using a wavelet transform-based hybrid model," *Energy*, vol. 193, Feb. 2020, Art. no. 116704.
[41] W. Qiao and Z. Yang, "Solving large-scale function optimization problem by using a new metaheuristic algorithm based on quantum dolphin swarm algorithm," *IEEE Access*, vol. 7, pp. 138972–138989, 2019.
[42] W. Qiao and Z. Yang, "Modified dolphin swarm algorithm based on chaotic maps for solving high-dimensional function optimization problems," *IEEE Access*, vol. 7, pp. 110472–110486, 2019.
[43] J. Chen, D. Lu, W. Liu, J. Fan, D. Jiang, L. Yi, and Y. Kang, "Stability study and optimization design of small-spacing two-well (SSTW) salt caverns for natural gas storages," *J. Energy Storage*, vol. 27, Feb. 2020, Art. no. 101131.
[44] W. Qiao, H. Lu, G. Zhou, M. Azimi, Q. Yang, and W. Tian, "A hybrid algorithm for carbon dioxide emissions forecasting based on improved lion swarm optimizer," *J. Cleaner Prod.*, vol. 244, Jan. 2020, Art. no. 118612.
[45] W. Qiao and Z. Yang, "An improved dolphin swarm algorithm based on kernel fuzzy C-means in the application of solving the optimal problems of large-scale function," *IEEE Access*, vol. 8, pp. 2073–2089, 2020.
[46] W. Qiao, Z. Yang, Z. Kang, and Z. Pan, "Short-term natural gas consumption prediction based on Volterra adaptive filter and improved whale optimization algorithm," *Eng. Appl. Artif. Intell.*, vol. 87, Jan. 2020, Art. no. 103323.
[47] H. Kandi, D. Mishra, and S. R. K. S. Gorthi, "Exploring the learning capabilities of convolutional neural networks for robust image watermarking," *Comput. Secur.*, vol. 65, pp. 247–268, Mar. 2017.
[48] L. Huang, "Watermarking algorithms for GIS vector data considering geometrical characteristics and topology relationships," Ph.D. dissertation, Nanjing Normal Univ., Nanjing, China, 2011.

XU XI received the B.S. degree from Zhengzhou University, Zhengzhou, China, in 2012, and the M.S. degree from Liaoning Normal University, Dalian, China, in 2015. He is currently pursuing the Ph.D. degree with the Department of Remote Sensing and Geographic Information Systems, Sun Yat-sen University, Guangzhou, China.

His research interests include geospatial data security and digital watermarking.

XINCHANG ZHANG received the B.S., M.S., and Ph.D. degrees from Wuhan University, Wuhan, China, in 1982, 1990, and 2004, respectively.

He is currently a Professor with the School of Geographical Science, GZHU, Guangzhou University, Guangzhou, China, and the Department of Remote Sensing and Geographic Information Systems, Sun Yat-sen University, Guangzhou. His research interests include geographic information systems, map synthesis, and geospatial data security.

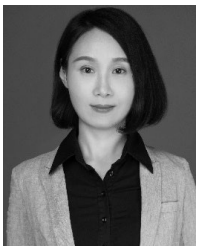

YING SUN received the B.S. degree in surveying and mapping from Chang'an University, Xi'an, China, in 2005, the M.S. degree in surveying and mapping from Wuhan University, Wuhan, China, in 2007, and the Ph.D. degree in geographical information science from Sun Yat-Sen University, Guangzhou, China, in 2014.

She was a Visiting Scholar with the Institute of Space and Earth Information Science, The Chinese University of Hong Kong, in 2018. She is currently an Associate Research Fellow with the School of Geography and Planning, Sun Yat-Sen University. Her research interests include high-resolution remote sensing, deep learning in remote sensing images, and ecology remote sensing.

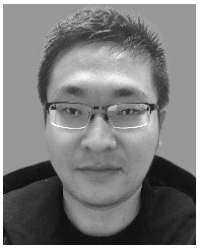

XIN JIANG received the B.S. degree from Hohai University, Nanjing, China, in 2017. He is currently pursuing the master's degree with the School of Geography Science and Planning, Sun Yat-sen University. His current research interests include mathematical modeling, high-performance computing, computer vision, and machine learning. In 2015, he won the first prize of the China Undergraduate Mathematical Contest in Modeling (CUMCM). He won the Honorable Mention of Mathematical Contest In Modeling (MCM/ICM), in 2016.

QINCHUAN XIN received the B.S. degree from Peking University, Beijing, China, in 2005, and the Ph.D. degree from Boston University, Boston, USA, in 2012.

He is currently an Associate Professor with the Sun Yat-sen University. His research interests include land surface remote sensing observation, geographic information systems, and multimedia security.